



Constraints on the Source of Short-Term Motion Adaptation in Macaque Area MT. I. The Role of Input and Intrinsic Mechanisms

NICHOLAS J. PRIEBE, MARK M. CHURCHLAND, and STEPHEN G. LISBERGER

Howard Hughes Medical Institute, Department of Physiology, W. M. Keck Foundation, Center for Integrative Neuroscience, and the Neuroscience Graduate Program, University of California, San Francisco, California 94143

Abstract

Neurons in area MT, a motion-sensitive area of extrastriate cortex, respond to a step of target velocity with a transient-sustained firing pattern. The transition from a high initial firing rate to a lower sustained rate occurs over a time course of 20–80 ms and is considered a form of short-term adaptation. The present paper asks whether adaptation is due to input-specific mechanisms such as short-term synaptic depression or if it results from intrinsic cellular mechanisms such as spike-rate adaptation. We assessed the contribution of input-specific mechanisms by using a condition/test paradigm to measure the spatial scale of adaptation. Conditioning and test stimuli were placed within MT receptive fields but were spatially segregated so that the two stimuli would activate different populations of inputs from the primary visual cortex (V1). Conditioning motion at one visual location caused a reduction of the transient firing to subsequent test motion at a second location. The adaptation field, estimated as the region of visual space where conditioning motion caused adaptation, was always larger than the MT receptive field. Use of the same stimulus configuration while recording from direction-selective neurons in V1 failed to demonstrate either adaptation or the transient-sustained response pattern that is the signature of short-term adaptation in MT. We conclude that the shift from transient to sustained firing in MT cells does not result from an input-specific mechanism applied to inputs from V1 because it operates over a wider range of the visual field than is covered by receptive fields of V1 neurons. We used a direct analysis of MT neuron spike trains for many repetitions of the same motion stimulus to assess the contribution to adaptation of intrinsic cellular mechanisms related to spiking. On a trial-by-trial basis, there was no correlation between number of spikes in the transient interval and the interval immediately after the transient period. This is opposite the prediction that there should be a correlation if spikes cause adaptation directly. Further, the transient was suppressed or extinguished, not delayed, in trials in which the neuron emitted zero spikes during the interval that showed a transient in average firing rate. We conclude that the transition from transient to sustained firing in neurons in area MT is caused by mechanisms that are neither input-specific nor controlled by the spiking of the adapting neuron. We propose that the short-term adaptation observed in area MT emerges from the intracortical circuit within MT.

INTRODUCTION

Our perception of the world is not based simply on sensory information currently available from our environment but also on the context in which we receive information. In the “waterfall” illusion, for example, long-term exposure to motion in one direction can induce the perception that a stationary stimulus is moving in the opposite direction (Schrater and Simoncelli 1998; Wohlgenuth 1911). Stimulus context affects our perception not only of

visual motion but also of the orientation of bars (Gibson and Radner 1937), the pitch of a sound (Stevens and Davis 1938), and the position of an object on the arm (Kilgard and Merzenich 1995).

Adaptation is a property of neuronal responses that may mediate the effect of context and recent sensory history on perception. In the visual system, adaptation can have many time courses ranging from the very long adaptation that produces the waterfall illusion to very short time scales that alter the discrimination of the direction of motion for a brief time (Takeuchi et al. 2001). On the time scale of tens of milliseconds, adaptation reduces the firing of visual neurons from an initial transient to a subdued sustained response. Retinal ganglion cells (Kaplan et al. 1993; Victor 1987), and many neurons in the lateral geniculate nucleus (Saul and Humphrey 1990) and primary visual cortex (V1), show a transient-sustained firing pattern for a step change in contrast (Kulikowski et al. 1979; Muller et al. 1999; Nelson 1991; Tolhurst et al. 1980), while neurons in visual area MT show a similar response pattern for a step change in target speed (Lisberger and Movshon 1999).

At least three classes of mechanisms could contribute to the short-time-scale adaptation that produces the transient response of MT neurons: 1) input-specific mechanisms: adaptation in MT could be inherited from adaptation already present in the firing of its inputs or could be created by short-term depression in the synapses that transmit those inputs to MT. 2) Intrinsic spiking mechanisms of individual neurons: many excitatory cortical neurons exhibit spike frequency adaptation for a step of input current so that the response consists of a transient that decays to a lower sustained firing rate. 3) Circuit properties: adaptation might result from processing that has occurred within MT or from feedback from areas higher in the hierarchy of visual motion processing. Of course, this third class of mechanism would depend on circuit properties in or beyond MT but would still have to be implemented by cellular mechanisms operating on MT neurons. The goal of the present pair of papers was to constrain the mechanisms of adaptations through extracellular recordings from MT neurons in anesthetized macaque monkeys. This first paper provides evidence that is inconsistent with explanations for adaptation based on both input-specific mechanisms from primary visual cortex to MT and intrinsic mechanisms related to the spiking of MT neurons.

METHODS

Physiological preparation

Extracellular single-unit microelectrode recordings were made in the middle temporal visual area (MT) of nine anesthetized paralyzed monkeys (*Macaca fascicularis*, *mulatta*) and a single awake, behaving monkey (*M. mulatta*) and the primary visual cortex (V1) of two anesthetized paralyzed monkeys (*M. mulatta*). A minority of the data were obtained from the awake animal and are shown primarily to emphasize the similarity of the results.

In acute experiments, anesthesia was induced with ketamine (5–15 mg/kg) and midazolam (0.7 mg/kg), and cannulae were inserted into the saphenous vein and the trachea. The animal's head was then fixed in a stereotaxic frame, and the surgery was continued under an anesthetic regime of isoflurane (2%) inhaled in oxygen. A small craniotomy was performed and the dura reflected, either directly above the superior temporal sulcus (STS) for recordings in area MT or above the occipital lobe for recordings in V1. The animal was maintained under anesthesia using an intravenous opiate, sufentanil citrate ($8\text{--}24 \mu\text{g} \cdot \text{kg}^{-1} \cdot \text{h}^{-1}$), for the duration of the experiment. To minimize drift in eye position, paralysis was maintained with an infusion of vecuronium bromide (Norcuron, $0.1 \text{ mg} \cdot \text{kg}^{-1} \cdot \text{h}^{-1}$). The animal was artificially ventilated with medical grade air. Body temperature was kept at 37°C with a thermostatically controlled heating pad. The electrocardiogram, electroencephalogram, autonomic signs, and rectal temperature were continuously monitored to ensure the anesthetic and physiological state of

the animal. The pupils were dilated using topical atropine and the corneas were protected with +2D gas-permeable hard contact lenses. Supplementary lenses were selected by direct ophthalmoscopy to make the lens conjugate with the display. The locations of the foveae were recorded using a reversible ophthalmoscope.

For recordings in area MT, tungsten-in-glass electrodes (Merrill and Ainsworth 1972) were introduced by a hydraulic microdrive into the anterior bank of the superior temporal sulcus (STS) and were driven down through the cortex and across the lumen of the STS into MT. The location of unit recordings in MT was confirmed by histological examination of the brain after the experiment, using methods described in Lisberger and Movshon (1999). For recordings in V1, the electrode was introduced just posterior to the lunate sulcus. After the electrode was in place, agarose was placed over the craniotomy to protect the surface of the cortex and reduce pulsations. Single units were isolated using a dual time-window discriminator (Bak Electronics, DDIS-1), and action potentials were amplified conventionally and displayed on an oscilloscope. Both a filtered version of the neural signals and a tone indicating the acceptance of a waveform as an action potential were played over a stereo audio monitor, and the time of each accepted waveform was recorded to the nearest 10 μ s for subsequent analysis. The recording sessions lasted between 84 and 120 h. The units included in this study are from 29 electrode penetrations in MT at different sites in nine monkeys and 24 penetrations in V1 in two monkeys.

Experiments on the awake monkey were conducted using an experimental and training protocol that has been described before (e.g., Lisberger and Westbrook 1985) in a monkey that had been trained to fixate spot targets. Eye movements were measured with the scleral search coil method (Judge et al. 1980), using eye coils that had been implanted with sterile procedure while the animal was anesthetized with isofluorane. In a separate surgery, stainless steel plates were secured to the skull and attached with dental acrylic to a cylindrical receptacle that could be used for head restraint. In addition, a craniotomy was performed over the STS and a cylinder was attached to the surface of the skull (Crist Instruments). During experiments, the head was immobilized by using a post to attach the implanted receptacle to the ceiling of a specially-designed primate chair. Microelectrodes were introduced through the cylinder into the cortex and lowered into area MT using the same approach as in the acute experiments. The animal was rewarded with juice for accurately fixating a target at the center of the display. Experiments were run daily, typically lasting 2–3 h.

All experiments in awake and anesthetized monkeys followed protocols that had received prior approval by the Institutional Animal Care and Use Committee at UCSF.

Stimulus presentation for acute experiments

After isolating a single unit in MT or V1, we mapped its receptive field on a tangent screen by hand. We recorded the spatial position of each single unit's receptive field and, for the majority of neurons, the size of the minimum response field. All of the neurons reported in this pair of papers had receptive field centers within 12° of the fovea.

After the receptive field location was determined, a mirror was positioned such that a random-dot texture on a display oscilloscope fell within the receptive field of the isolated neuron. Visual stimuli were then presented on an analog oscilloscope (Hewlett-Packard models 1304A and 1321B, P4 phosphor), using signals provided by D/A converter outputs from a PC-based digital signal processing board (Spectrum Signal Processing). This system affords extremely high spatial and temporal resolution, allowing a frame refresh rate of 500 or 250 Hz and a nominal spatial resolution of 64,000 \times 64,000 pixels. The apparent motion created by our display is effectively smooth at these sampling rates (Churchland and Lisberger 2001; Mikami et al. 1986). The display was positioned 65 cm from the animal and subtended 20° horizontally by

20° vertically. Experiments were performed in a dimly lit room. Due to the dark screen of the display, background luminance was beneath the threshold of the photometer, less than 1 mcd/m².

Experiments consisted of a sequence of brief trials with an inter-trial interval of about 700 ms. All trials began with the appearance of a stationary, uniform random dot texture (0.75 dots/°²). Because many neurons in MT respond better if the moving texture is surrounded by a field of stationary dots, we used two nonoverlapping textures of the same dot density. A surround texture remained stationary for the duration of the trial, while a texture in the center of the screen moved. For all trials, the textures appeared and were stationary for 256 ms before starting to move. After the motion was completed, the dots remained visible for an additional 256 ms. Motion in the center texture was used to characterize the preferred direction by moving the texture in eight directions for either 512 or 256 ms. After the preferred direction was identified, the preferred speed of the neuron was measured by moving the center texture in the preferred direction at speeds of 0.125, 0.25, 0.5, 1, 2, 4, 8, 16, 32, 64, and 128°/s.

After texture direction and speed had been optimized for the neuron under study, we conducted an iterative recording procedure to center the receptive field on our display. We divided the center texture into small units that were either 2 or 4° across and measured the response of the neuron for motion of each small texture. We then determined the spatial extent of the receptive field using an on-line analysis routine and, if necessary, adjusted the mirror to better center our visual stimulus on the neuron's receptive field. If the position of the mirror had been changed, we once again determined the spatial extent of the receptive field on our monitor. Because the response strength of many neurons in area MT depends on the size of the moving texture (Allman et al. 1985a,b), we also optimized the size of the texture by adjusting the center and surround textures so that that moving texture subtended 2.5, 5, 10, 15, and 20°. Once we were satisfied that the stimulus had been optimized for the response preferences of the neuron under study, we conducted the experiments described in Results.

Stimulus presentation for awake animal

The presentation of stimuli for the awake animal was similar. Minor differences were: dot density in the textures was 0.25 dots/°²; the moving textures were not surrounded by a field of stationary dots; instead of using anesthesia and paralysis to prevent the eyes from moving, recordings were made while the monkey fixated a stationary spot and ignored the motion of the eccentric texture. Fixation was excellent, so that smooth eye motion under such conditions was minimal, on the order of 1% of the stimulus speed (see Churchland and Lisberger 2001, *monkey M*, for a full analysis).

Data acquisition and analysis

Experiments were controlled by a computer program running on a UNIX workstation and a Windows NT PC running the real-time extension RTX (VenturCom). The two computers were networked together: the UNIX workstation provided an interface for programming target motion and customizing it during recording from a neuron, while the PC provided real-time control of target motion and data acquisition. The times of spikes were recorded by the PC and sent over the network to the UNIX workstation, which combined them with codes indicating the target motion that had been commanded and stored both for subsequent analysis. For the recordings made in the awake monkey, analog voltages proportional to horizontal and vertical eye position and eye velocity were sampled at 1,000 Hz on each channel and stored for subsequent verification of good fixation.

In both anesthetized and awake recordings, each experiment consisted of a list of trials, where each trial presented a different target motion. A different seed was used to create the

pseudorandom sequence of initial dot positions in each trial. As a result, every trial presented a different texture, even for repetitions of the same target motion. Trials were sequenced by shuffling the list and presenting the trials in a random order until all the trials in the list had been presented. The list was then shuffled and repeated again until enough repetitions of each stimulus had been obtained. In the awake recordings, the monkey was required to fixate a stationary spot with an accuracy of 2° . If the monkey broke fixation, the trial was aborted and placed at the end of the list to be presented again before the list was shuffled and repeated.

Data were analyzed by aligning all the responses to identical trajectories of target motion on the onset of target motion and accumulating poststimulus time histograms with a binwidth of 1 ms. For the purposes of presentation, the histograms were built with a binwidth of 8 or 16 ms. Background responses were eliminated by creating a histogram for trials that presented a stationary stimulus, computing the mean firing rate during the interval when other stimuli were moving, and subtracting this scalar from the firing rate in every bin of every other histogram. We then measured firing rate from the background-corrected histograms to determine the stimulus selectivity of each neuron and to quantify the results of each experiment. Specific analyses are presented at the relevant places in Results.

To determine whether neurons should be included in our analysis, we estimated the directional selectivity using a directional index (DI)

$$DI = 1 - \frac{R_N}{R_P} \quad (1)$$

where R_P is the response elicited by motion in the preferred direction of the neuron and R_N is the response elicited by the direction 180° away from the preferred direction. R_P and R_N were measured as the mean firing rate during the 512-ms interval of texture motion. We considered neurons to be direction selective and included them in our report if the value of DI was more than 0.5. This included all 213 neurons we recorded in area MT and 63 of the 393 neurons we sampled in V1.

For the analysis shown in the final section of Results, it was important that the excitability of the neuron did not change over the course of the recording. To assay whether a neuron's responses were stationary, we measured the number of spikes recorded during the period 150–250 ms after motion was initiated for each presentation of motion in the preferred direction. We then fit first-, second-, and third-order polynomials to the number of spikes found in the sequence of trials, ordered by the time of stimulus presentation

$$y = bt + a \quad (2)$$

$$y = ct^2 + bt + a \quad (3)$$

$$y = dt^3 + ct^2 + bt + a \quad (4)$$

After making each fit, we computed 95% confidence intervals for each parameter b , c , or d of the models. If the confidence intervals for b , c , or d indicated a statistically significant deviation from 0, then the neuron was discarded from further analysis.

RESULTS

Properties of transient responses in MT neurons

Many neurons in area MT undergo a short-term adaptation that shapes the temporal dynamics of their response to moving stimuli (Lisberger and Movshon 1999). As illustrated in Fig. 1A,

the average response to a step of target speed consists of an initial transient followed by a rapid decrease to a sustained firing rate that remains steady for the duration of the motion. The transient represents the unadapted response of the neuron to motion, while the sustained phase represents the adapted response of the neuron.

To describe the time course and amplitude of the adaptation we sought to understand, we begin with a thorough analysis of the transition from the transient high firing rate to the lower sustained responses of MT neurons and the time-dependent recovery from adaptation. For each MT neuron we recorded with a transient response, we made histograms like that in Fig. 1A describing the time average of the response to steps of target velocity of the neuron's preferred direction and speed. We then fit the transition from transient firing to sustained firing with single exponentials of the form

$$R(t) = f_{\text{sus}} + (f_{\text{max}} - f_{\text{sus}})e^{-t/\tau} \quad (5)$$

where f_{sus} is the firing rate during the sustained portion of the response, f_{max} is the peak firing rate, and τ is the time constant of the exponential. Fits were made over a 200-ms interval starting from the peak of the neuron's response. Equation 5 typically provided an excellent fit to our data, as shown by the solid curve overlying the histogram in Fig. 1A. Using the parameters from the fits, we defined the transient-sustained ratio (TSR) as

$$\text{TSR} = \frac{f_{\text{max}}}{f_{\text{sus}}} \quad (6)$$

The onset of adaptation varied extensively among neurons and is summarized in Fig. 1, B and C. The time course of the onset of adaptation, reflected in the decay in firing from the transient to sustained response, had a time constant that ranged from 8 to 85 ms (Fig. 1B) with a mean of 25.9 ms. The transient-sustained ratio ranged from 1.23 to 21, with a mean of 2.61 and a median of 2.53 and was not significantly correlated with the time constant of the decay of firing from the peak of the transient to the sustained rate (Fig. 1C) or with the transient firing rate.

To assess the time course of recovery of the neuron from its adapted state, we used a condition/test paradigm that consisted of sequential presentation of two stimulus motions. We measured the effect of the initial motion (the conditioning motion) on the neuron's response to the subsequent motion (the test motion). If the conditioning motion did not cause adaptation, then the response to the test stimulus would be the same as if there had been no conditioning motion at all: the neuron would display its stereotypical transient firing rate. If the conditioning stimulus did adapt the neuron, then the transient response to the test stimulus would be reduced: reduction to the level of the sustained rate would represent maximal adaptation.

In the experiments used to demonstrate the temporal properties of the recovery from adaptation, the conditioning and test motions were delivered at the same locations in the receptive field and were always of the direction and speed that drove the largest response of the neuron. The response to each test motion was calculated by subtracting the response to conditioning motion alone from the response to conditioning/test motion. We initially used conditioning and test motions that were only 64 ms in duration because these seemed sufficient to document the adaptation of a transient with a duration less than 64 ms: subsequent experiments use longer duration motions and demonstrated that the adaptation is specific to the transient response.

The recovery from adaptation is shown in Fig. 2A for an example MT neuron. When the test motion occurred immediately after the end of the conditioning motion (traces labeled CTI = 0), the response to the conditioning/test motion (histogram) followed the response to the conditioning motion (bold, continuous trace) nicely in the first half of the response before the

response to the test motion would have begun. In the second half of the response, which should have been driven by the test motion, the response to conditioning/test motion was only slightly larger than that to the conditioning motion alone, indicating that the response to the test motion was strongly attenuated. As the conditioning/test interval (CTI) increased from 32 to 64 ms and eventually to 256 ms, the size of the response to the test motion gradually recovered. We quantified the time course of the recovery from adaptation by measuring the difference in mean firing rate between the responses to the conditioning/test stimulus and the test stimulus alone during the 64-ms interval starting 64 ms after the onset of the test motion. Plotting this difference firing rate as a function of the CTI (Fig. 2B) revealed that recovery was complete for this example neuron within 256 ms and was fit well by an exponential with a time constant of 73 ms (continuous curve in Fig. 2B). We measured the time constant of recovery from adaptation for 86 MT neurons and found a broad distribution with a mean of 86 ms (median = 78 ms) as shown in the histogram of Fig. 2C.

Lisberger and Movshon (1999) linked adaptation to the transition from transient to sustained response by showing that the amount of adaptation demonstrated by two-step stimuli was strongly correlated with the transient-sustained ratio of the neuron under study. We obtained the same strong correlation in our larger sample of neurons. Lisberger and Movshon (1999) also found that the adaptation demonstrated in Fig. 2 was very similar when the conditioning motion was a step of target speed with a duration of 512 ms, implying that brief motion was sufficient to fully adapt the neural response. In the present series of two papers, we have taken advantage of the same experimental design to probe the stimulus selectivity of the adaptation. We have systematically varied the visual properties of the conditioning motion while probing the adaptation with a test motion consisting of the preferred stimulus for the neuron under study.

Experimental design for evaluating input-specific mechanisms of adaptation

Two input-specific mechanisms could account for the adaptation observed in area MT: short-term depression of the efficacy of synapses that provide input from V1 to area MT (Chance et al. 1998; Kayser et al. 2001) or adaptation occurring at the level of V1 and simply replayed in area MT. To investigate whether either of these input-based mechanisms underlies the adaptation observed in area MT, we took advantage of the fact that the receptive fields of MT neurons are large in comparison to those of V1 neurons at corresponding eccentricities and the common assumption that MT neurons have larger receptive fields because they pool the responses of neurons in V1 that have different receptive field locations. We performed condition/test experiments in MT using small textures designed to stimulate two different sets of inputs from V1 to MT. We induced adaptation with conditioning motion in one part of the receptive field of an MT neuron and probed adaptation with test motion in a different part of the receptive field. If adaptation in MT occurs in the input pathway from V1 to MT, then adaptation should not transfer from one portion of an MT receptive field to another. If adaptation is derived from mechanisms that operate within area MT, then adaptation should transfer from one location to another within a single MT receptive field. In the next sections of Results, we demonstrate that adaptation in area MT transfers between spatial locations that activate different neurons in V1. We also confirm that the motion adaptation present in MT neuron responses is not present in the direction-selective neurons in V1.

Spatial transfer of adaptation in MT neurons

Figure 3 illustrates the results of an experiment that tests the spatial extent of the transfer of adaptation. First, we mapped the receptive field of each of 67 neurons in area MT by placing small ($4 \times 4^\circ$) textures at 25 different locations on our display and measuring the response to motion across each location. These responses are summarized in the histograms at each of the 25 locations in Fig. 3A and in the continuous map derived in Fig. 3B. All of our neurons had

receptive field centers located within 10° of the fovea (Fig. 3A, \times), and their receptive fields typically covered 2×2 or 3×3 of the small textures used for mapping. After the spatial extent of the neuron's receptive field had been determined, we chose two locations that were separated by at least 2° (1.2° in awake animals) and where motion excited the neuron approximately equally. For the neuron used to create Fig. 3, the locations of the two textures are indicated by the gray and black dashed boxes. Corresponding black and gray bars have been placed below the histograms in Fig. 3, C–H, to indicate the times when each of the stimuli was moving. At their closest point, the distance between the two textures was 2.6° . Because the center of the receptive field for this neuron was 6° from the fovea, 2.6° is about four times larger than one receptive field width in area V1.

Figure 3, C and D, shows that the neuron had similar responses to motion in each patch alone: large transients followed by sustained firing. When motion of the adapting stimulus at the gray site was followed immediately by motion of a test stimulus at the black site (histogram in Fig. 3E), the early part of the response matched the response to the adapting stimulus presented alone (thick gray trace in Fig. 3E). The later part of the response, which was driven by the motion of the test stimulus, failed to show a second transient, and the firing rate simply continued at approximately the sustained level from the early part of the response. To isolate the response to the test motion after adaptation, we subtracted the response to the conditioning motion (Fig. 3C) from the response to the sequence of conditioning and test motions (Fig. 3E). The resulting “difference” histogram (Fig. 3G) reveals that the response to the test motion consisted of a small sustained response without any transient. For comparison, the response to the test motion without prior adaptation had a large transient (Fig. 3D). Figure 3, D, F, and H, shows the results of the same analysis when the presentation order was reversed so that motion at the black location provided the conditioning stimulus and motion at the gray location the test stimulus. The difference histogram (Fig. 3H) again revealed that the isolated response to the test motion after adaptation had only a small transient response and was very different from the control response to the same motion (Fig. 3C).

Adaptation in one spatial location significantly reduced the amplitude of the transient response to motion in another location for most of the neurons in our sample population. We quantified this effect by comparing the transient-sustained ratio of each neuron in the absence and presence of conditioning motion. We used Eq. 6 to compute the transient-sustained ratio, but we obtained the values of f_{\max} and f_{sus} by measurement from the difference firing rates calculated as illustrated in Fig. 3, G and H. f_{\max} was taken as the peak response in any 32-ms interval within 150 ms after test motion began; f_{sus} was defined as the average firing rate during the period 150 to 250 ms after the motion in the test location began. In Fig. 4A, all MT neurons lie below the line of slope 1, indicating that the adaptation from the conditioning motion at one site caused a decrease in the transient-sustained ratio for a test motion at another site. The decrease was statistically significant in 52 of the 67 MT neurons tested in this experiment (filled symbols, $P < 0.05$, paired t -test) and was clearly present in neurons recorded in both anesthetized (squares) and awake (triangles) monkeys. We did not test for differences between neurons recorded in these two preparations because we could not compensate for effects of differences in the exact stimulus conditions and in the criteria for selecting neurons for study.

The degree of the transfer of adaptation from motion in one spatial location to another was quantified further by computing the transient index (TI) as

$$\text{TI} = \frac{R_{\text{test|condition}} - R_{\text{sustained}}}{R_{\text{transient}} - R_{\text{sustained}}} \quad (7)$$

where $R_{\text{transient}}$ and $R_{\text{sustained}}$ are the transient and sustained responses of the neuron to the test motion without preceding adaptation, and $R_{\text{test|condition}}$ is the transient response to the test

motion after presenting conditioning motion in another portion of visual space. As before, measurements were taken from the difference firing rates (e.g., Fig. 3, *G* and *H*). TI would be zero if the response to the test motion did not contain a transient response and was only composed of the adapted, sustained level of firing. TI would be one if the transient response to the test motion was the same with or without preceding conditioning motion. For the neuron illustrated in Fig. 3, TI was -0.24 and 0.32 when the test motion was in the locations indicated, the black and gray bars and squares, respectively. Across our sample, there was a broad range of values of TI (Fig. 4*B*), and the mean TI was 0.23 . Thus the adaptation induced by conditioning motion in one portion of the receptive field caused, on average, a 77% reduction ($100 \times [1.0 - 0.23]$) in the amplitude of the transient caused by subsequent test motion at a different location.

Motion in the conditioning patch had a much smaller effect on the sustained firing rate evoked by the test motion (Fig. 4*C*). For this measure, the points plotted much closer to the line of slope one, and the difference was statistically significant in only 6 of 67 MT neurons (\blacksquare , $P < 0.05$, paired *t*-test). Thus adaptation induced by motion at one site altered selectively the transient response to motion at a different site.

The data in Fig. 4 were computed after isolating the adapted response to the test motion by computing the difference between the firing rate evoked by the conditioning/test motion and the firing rate evoked by the conditioning motion alone (as in Fig. 3). This subtraction ought to be the correct way to isolate the adapted response because it removes the tail of firing rate that is related to the end of the conditioning motion and reveals the onset of the response to the test motion. However, it also incorporates an assumption of linearity in the responses of the neurons and might underestimate the true value of TI. To place an upper limit on the size of the transient response to the test motion after adaptation, we also computed TI from the response to conditioning motion followed by test motion without subtracting the response to conditioning motion alone. We made the measurement at the same latency used for the measurements that appear in Fig. 4. For this conservative estimate of the effect of conditioning motion on test response, the mean value of TI was 0.47 . We conclude that the adaptation induced by conditioning motion in one portion of the receptive field caused at least a 53% reduction in the amplitude of the transient caused by the subsequent test motion at a different location and probably as much as a 77% reduction.

Time course of recovery from adaptation in MT neurons

In 24 neurons, we studied the time course of recovery from adaptation to ask whether the recovery followed the same time course when the test and conditioning motions were in different locations as it did when they were in the same location (Lisberger and Movshon 1999). The data in Fig. 5 show an example of the histograms accumulated for one neuron in this experiment. These experiments were similar to those in Fig. 2 in that we varied the interval between the offset of the conditioning motion and the onset of the test motion. However, conditioning and test motions were 256-ms duration (instead of 64 ms) and appeared in separate spatial locations in the visual field. As expected, Fig. 5*A* shows that the transient response to the test motion was strongly attenuated when the CTI between the end of the conditioning motion and the start of the test motion was zero, but the conditioning motion did not cause any effect on the sustained response to subsequent test motion. The transient response recovered gradually as the CTI was increased from 32 to 256 ms.

To summarize the recovery from adaptation, for each of the 24 neurons tested, we measured the TI from the difference firing rate (conditioning/test minus conditioning motion alone) at each CTI. We then fit the relationship between TI and CTI with an exponential of amplitude 1.0 to measure how quickly the transient response of each neuron recovered. For each neuron, we compared the time constant of recovery for conditioning/test motions at different spatial

locations with that for conditioning/test motions at the same spatial location. With the exception of a few neurons, we found good general agreement between the time constants of recovery for conditioning/test stimuli at the same versus different locations (Fig. 5B). Four of the five exceptions recovered much faster for conditioning/test stimuli at the same location than they did for conditioning/test stimuli at different locations. These exceptions might be the reflection of different mechanisms of adaptation for the conditioning/test stimuli at the same versus different locations, but might also result from the use of different durations of the conditioning and test motions for the different experiments. Overall, the similarity in the recovery from adaptation favors the conclusion that there is a common underlying mechanism of adaptation that operates across the spatial extent of the receptive field.

Comparison of receptive and adaptation fields in MT neurons

We define the receptive field as the part of the visual field in which test motions alone evoked responses in the neuron, and we define the adaptation field as the part of the visual field where conditioning motion caused a reduction in the transient response to subsequent test motion near the center of the receptive field. To measure the adaptation field of the neuron, conditioning motion was placed at different spatial locations around a central test location. For five neurons, we used eight conditioning motion locations surrounding the center of the response field at a single distance. For the neuron illustrated in Fig. 6 and for eight other neurons, we used 24 different conditioning locations at three distances and eight angles relative to the testing location in the center of the receptive field. The five histograms in Fig. 6, A–E, show the results for five of these conditioning motion locations. In Fig. 6, A and E, the conditioning location (bold square) was entirely outside the receptive field (dashed circle), and the response to the motion at the test location (less bold square) showed a large transient even when the test motion immediately followed the conditioning motion. However, when the conditioning motion was placed inside the receptive field of the MT neuron, there was a reduction in the amplitude of the transient evoked by the test motion (Fig. 6, B–D). The reduction was most complete for the conditioning motion location that evoked the largest response itself (Fig. 6C).

Each neuron's adaptation field was constructed by measuring the effect of the location of conditioning motion on the transient response to the test motion. To summarize the results of this experiment for each neuron, we created graphs such as that in Fig. 6F. This graph plots the transient index measured for each conditioning motion location versus the response evoked by the conditioning motion at that location. The latter was quantified by measuring the average firing rate over the interval from 150 to 250 ms after the onset of the conditioning stimulus. For the neuron illustrated in Fig. 6, the amount of adaptation was closely related to the size of the response evoked by the adapting stimulus alone. There was an inverse relationship between the transient index and the response to the conditioning motion (correlation coefficient of -0.82). The same result was obtained in all 14 neurons we studied, with all but 1 neuron showing correlation coefficients between -0.4 and -1.0 (Fig. 6H) that were statistically significant (2-tailed t -test, $P < 0.05$). In Fig. 6F, we have emphasized the relationship between the amount of adaptation and the response caused by conditioning motion, but it is also important to note a number of sites that plot at 0.0 on the x axis but below 1.0 on the y axis. These points represent conditioning motion locations that evoked little or no response but still caused substantial adaptation of the response to the testing motion.

To quantify the sizes of the receptive and adaptation fields, we fit each with two-dimensional Gaussian functions with the same value of σ along each axis (Britten and Heuer 1999). These are summarized in Fig. 6G, which shows contour plots derived from the Gaussian fits to the response to the conditioning motion (continuous contours) and to 1 minus the transient index (dashed contours) for the same neural responses shown in the *top panels*. The two contour plots

are centered at the same location. However, the adaptation field was larger than the receptive field for the neuron illustrated in Fig. 6: for each contour value (e.g., 0.9, 0.6, and 0.3), the contour for adaptation lies outside that for the response evoked by the conditioning motion itself. We observed the same result for all 14 neurons tested in this experiment: in a plot of the value of SD used for the Gaussian fit for adaptation as a function of that for the response (Fig. 6*I*), each neuron plotted above the line of slope 1. However, the adaptation field was never more than two times the size of the receptive field for the 14 neurons we studied in area MT. Thus adaptation in MT is on a spatial scale that is slightly larger than that of the receptive fields in MT.

Absence of spatial transfer of adaptation in V1

Can the large spatial scale of adaptation in MT be attributed to a similar scale of adaptation in V1? Many researchers have shown that the responses of V1 neurons to stimuli inside their receptive fields can be modified by stimuli outside their receptive fields (Cavanaugh et al. 1998; Hubel and Wiesel 1965; Knierim and van Essen 1992; Walker et al. 1999; Zipser et al. 1996). We therefore measured the effect of conditioning motion outside the receptive field on responses to motion inside a V1 receptive field. Stimuli presented to V1 neurons were comparable to those used in MT: direction tuning was assessed with the motion of a $5 \times 5^\circ$ dot pattern with a dot density of 0.75 dots/ $^\circ^2$. Of the 393 V1 neurons we isolated, we restricted our analysis to the 63 neurons whose directional index exceeded 0.5 (see Methods). As previously reported (Movshon and Newsome 1996), the majority of the direction-selective neurons were found either directly above layer 4 or in layer 6 of cortex. The center of the receptive fields of the neurons recorded from in V1 varied from 1 to 5° eccentric, and the receptive field diameters were less than 1° .

The design of the conditioning/test experiment was the same in V1 as it had been in MT. First, we measured the responses of V1 neurons to test motion placed directly in the receptive field of the neuron (fine dashed box at center of Fig. 7*A*) and moving in the neuron's preferred direction and speed. Next, we measured the response of the neuron to test motion immediately preceded by conditioning motion in one of eight locations surrounding the test motion (bold dashed boxes in Fig. 7*A*). The locations of the conditioning motion were not customized for the size of the V1 receptive fields but rather were the same locations used for conditioning motion in recordings from neurons in MT: a separation of at least 1.2° was maintained between the conditioning and test motions. We were able to record responses in the conditioning/test experiment from 39 of the 63 direction-selective neurons. We studied only direction-selective neurons because these are the neurons that project from V1 to MT (Movshon and Newsome 1996).

Direction-selective neurons in V1 did not show any consistent adaptation when test motion within the receptive field was applied immediately after conditioning motion outside the classical receptive field. For example, the V1 neuron shown in Fig. 7*B* had a typical response profile: a large response to the test motion alone (Fig. 7*B*, center) and an equally large response after conditioning motion at eight surrounding locations (Fig. 7*B*, surrounding histograms). In each of the eight surrounding histograms, the conditioning motion, presented at times indicated by the bold horizontal bars below the histograms, also failed to cause any response because it was out of the receptive field. Note also that the neuron illustrated in Fig. 7*B* responded with a brief burst of spikes after the appearance of a stationary texture well before any part of the texture began to move. This neuron's response is typical of the responses found in V1 in that it lacks the transient response that is observed in area MT. Figure 7*C* shows results for the V1 neuron that showed the largest transient response in our sample. Again, responses to test motion were not significantly altered by the presence of preceding motion outside the classically defined receptive field.

To quantify the effect of conditioning motion outside the classical receptive field on the response of V1 neurons to test motion inside the receptive field, we again isolated the response to the test motion by subtracting the response to the conditioning motion along from that for each conditioning/test stimulus. We then measured the peak firing rate in a sliding 32-ms bin for the test motion alone and for the isolated responses to test motion after conditioning motion in each location. In the polar plots we used to summarize these data (Figs. 8, *A* and *B*), the dashed circles indicate the 95% confidence intervals (mean \pm SE) for the peak firing rate during test motion alone. Each symbol shows the response for test motion following conditioning motion at a single location, with the symbol plotted at an angle indicating the location of the conditioning motion, and a distance from the center of the graph indicating the peak firing rate. For these two neurons, and all other neurons, the effects of conditioning motion on the test response were small and irregular. To assess whether the effect of conditioning motion on the test response was statistically significant, we did paired *t*-tests for each set of conditioning and test motion. Given that eight different comparisons were made, we used a criterion of $P < 0.018$ to determine significance (Bonferroni's correction, correlation = 0.5) (Miller 1981), instead of the usual $P < 0.05$. Neither of the units shown in Fig. 8, *A* and *B*, and only 2 of the 39 neurons in our population, showed significant effects of conditioning motion at any location using this criterion.

It is possible that adaptation might be consistently present in a restricted location, but not reach statistical significance in tests based on all conditioning locations. To evaluate this possibility, we analyzed the data in two additional ways. 1) To test for a significant effect of the position of the conditioning stimulus, we used circular statistics (Rayleigh's test) to test for an effect of location of the conditioning stimulus (Batschelet 1981). This analysis revealed the 3 of 39 neurons had statistically significant effects of conditioning location. The effects were all small. 2) To test for a relationship between the site of an effective conditioning stimulus and the preferred direction of the neuron, we rotated the polar graphs for all 39 neurons we studied so that the conditioning site located in the preferred direction of motion relative to the center of the receptive field was plotted to the right. We then normalized each response by the response of the same neuron to the test motion alone and averaged. This revealed a uniform distribution with a normalized transient response amplitude of one at every site of conditioning motion (open triangles Fig. 8C).

Input-specific adaptation might not be excluded by our data if the inputs from V1 neurons were organized so that the spatial locations of maximum adaptation in V1 were aligned in the inputs from V1 to each MT neuron. To determine the maximum adaptation that could arise from this organization, we rotated the polar plots so that the conditioning location that induced maximal adaptation of the test response was plotted to the right. We then normalized each neuron's responses for the maximum and averaged across neurons. This revealed about 40% adaptation of the transient response at the site of the maximal adaptation, normalized transient response amplitudes close to one at all other sites, and a hint of enhancement at the conditioning locations opposite to the maximal adaptation (open triangles, Fig. 8D). We think that the reduction of the transient response at one location in Fig. 8D results from response variability rather than from conditioning. If it were caused by conditioning, then conditioning motion at neighboring locations also should have caused adaptation. We therefore conclude that the spatial extent of adaptation in V1 is limited to the classical response field.

Quantitative comparison of adaptation fields of MT and V1 neurons

Figure 8, *C* and *D*, also plots the results of the same analyses described in the preceding text, of the spatial extent of adaptation, for MT neurons. When the adaptation fields were rotated so that the preferred direction of motion was to the right (Fig. 8C), MT neurons (filled circles) showed approximately the same adaptation for all locations of the conditioning motion and

much more adaptation than did V1 neurons (open triangles) at all locations. When the adaptation fields were rotated so that the location of the conditioning motion causing the largest adaptation was plotted to the right (Fig. 8D), MT neurons (filled circles) showed the largest adaptation for the conditioning location, as expected given the way the graph was created, and as found for V1 neurons (open triangles). However, MT neurons showed adaptation at all other locations of conditioning motion, while V1 neurons did not.

Absence of transient responses to motion onset in V1 neurons

Most direction-selective V1 neurons did not show the transient response to a step of target speed that is the signature of adaptation in MT. To quantify the apparent difference, we used a stimulus consisting of a $5 \times 5^\circ$ patch of dots moving with the preferred direction and speed of the V1 neuron under study and measured the transient-sustained ratio. Figure 9 shows histograms from five V1 neurons and five MT neurons. While a few V1 neurons responded with small transients to the onset of stimulus motion (e.g., Fig. 9A, top left histogram), the majority of V1 neurons did not show transient responses. Neurons were chosen for illustration in Fig. 9 by ordering them according to the value of transient-sustained ratio. The histograms at the top of each column show the responses of the neurons that had the largest transient-sustained ratio in our sample from V1 and MT, while the third histograms in each column approximate the median response.

Figure 10B summarizes the difference in the distribution of transient-sustained ratios in V1 and MT. As before, transient-sustained ratio was calculated by Eq. 6: f_{\max} was taken as the peak response in any 32-ms interval within 150 ms after motion began; f_{sus} was defined as the average firing rate during the period 150 to 250 ms after the motion began. One V1 neuron had a transient-sustained ratio more than 2 and a few had transient-sustained ratios as high as 1.4. However, the population of V1 neurons is grouped around a transient-sustained ratio of 1 with a mean value of 1.02. For MT neurons, transient-sustained ratios could be larger than 6 and the mean value was 1.93. The lack of transient responses to the onset of motion in V1 neurons may be surprising, since there are many reports of transient responses to flashed stimuli (Muller et al. 1999; Nelson 1991; Tolhurst et al. 1980). The lack of transient responses for our stimuli may be a result of using a low dot density of 0.75 dots/ $^\circ^2$: V1 neurons may have only responded when an individual dot crossed their receptive fields. Because the dot texture for each presentation was randomly changed, the time that a dot would cross the receptive field of a V1 neuron would be different for each trial. Whatever the basis for the lack of transient response to the onset of motion, direction-selective neurons in V1 do not show the transient firing that is observed in MT when they are tested with the same visual stimuli.

Direct test of intrinsic spiking-related mechanisms of adaptation

The previous sections showed that the amount of adaptation of MT neurons responses caused by conditioning motion at a given site in the receptive field was related to the size of the response caused by the conditioning motion. However, data presented so far do not distinguish whether the adaptation was a direct effect of the neuronal response or if the key factor was the location of the conditioning motion relative to the center of the receptive field. This is a subtle difference in terms of phenomenology but a critical one in terms of constraining the mechanism of adaptation in MT.

To assay whether the neuron's own activity causes adaptation, we used two approaches that took advantage of the trial-by-trial variability of the response during the initial transient (Softky and Koch 1992). For each neuron, we first defined a transient interval starting at the onset of the response and having a duration set to the time constant of the decay of firing rate from Eq. 5 (vertical dashed lines for an example neuron in Fig. 10A), and a subsequent interval as the next 16 ms. We then counted the number of spikes in each of these two intervals for every trial

and asked if they were correlated. If short-term adaptation results from the neuron's own activity, then the number of spikes in the subsequent interval should be related to the number of spikes in the transient interval. Figure 10B uses the size of each symbol to indicate the number of instances of a given combination of number of spikes in the transient (x axis) and subsequent (y axis) intervals. Spike counts in the transient interval ranged from zero to five, but there was not a strong relationship between the number of spikes during the transient interval and the subsequent interval. The correlation coefficient was 0.13 and was not significantly different from zero (t -test, $P > 0.05$) (Sokal and Rohlf 1995).

We recorded a sufficient number of repeats of the preferred stimulus (more than 65) to perform this analysis in 66 neurons. However, only 35 of the 66 neurons were admitted for the analysis by the criterion that their excitability remained stationary for the recording period (see Methods). It is important that the neuronal response remain stationary for the duration of the recording because such fluctuations in excitability can cause inaccurate overestimates of correlations. The histogram in Fig. 10C shows that the distribution of correlation coefficients was centered near zero and only two neurons had statistically significant, positive correlations (filled histogram bar).

We used a second analysis to demonstrate directly that the transition from transient to sustained firing is not produced by a neuron's own spikes. If spikes caused adaptation, then for trials in which there were no spikes produced during the transient interval, the firing rate should be higher in the subsequent interval. The transient should simply be delayed. Figure 11A shows the distribution of spike counts during the transient interval for the same neuron whose data are shown in Fig. 10, A and B. Of 265 trials, there were 26 trials in which no spikes were observed during the transient interval. Figure 11B shows the response histogram created for those 26 trials. Following the period in which there were no spikes, the response of the neuron followed very nearly the average response for all other trials. The lack of a large delayed transient indicates that the neuron has undergone adaptation during the transient period despite not having produced any spikes. The response of the neuron following the transient period also indicates that the neuron was capable of a normal response and was not somehow impaired during that trial.

We were able to perform this analysis for 25 neurons that had at least four trials with no spikes during the transient period. For each neuron, we computed the mean firing rate for the 16-ms interval immediately after the initial transient period separately for trials with and without firing in the transient period. In general, the firing rate after a transient interval with spikes was the same or higher than the firing rate after a transient interval without spikes so that most points in Fig. 11C plot above the line of slope one. The effect of the presence or absence of spikes in the transient interval on subsequent firing was statistically significant in 4 of the 25 neurons (Fig. 11C, filled symbols). In each instance, these neurons had a higher firing rate after the transient period when there were spikes during the transient period, the opposite of the result predicted if spikes in the transient interval cause short-term adaptation.

One final prediction of adaptation based on intrinsic spiking mechanisms in MT neurons would be that the background firing rate after the stimulus might be depressed relative to before the stimulus. We tested this prediction in 30 neurons with background firing rates of more than 5 spikes/s and found no evidence of a change in the background response after stimulation. Further the ratio of background firing rate after the stimulus divided by background firing rate before the stimulus was not related to the transient/sustained ratio of the neuron.

DISCUSSION

Many neurons in the visual system exhibit transients at the onset of their preferred stimulus. In MT, the transients are present at the onset of motion of a stimulus that was present but stationary before it started to move, but are not present when the same stimulus stops moving (Lisberger and Movshon 1999). The transient is not simply a response to the onset of visual stimulation and is also not a response to the contrast flash associated with a sudden change in the speed of motion. Instead, our data, along with the prior report of Lisberger and Movshon (1999), have shown that the transient response of MT neurons is tightly linked to the presence of a form of short-term adaptation. The short-term adaptation has been demonstrated by a series of condition/test experiments in which the conditioning motion of a preferred stimulus suppressed the response to a subsequent test motion. The transient responses in MT can be understood as the signature of an adaptation mechanism that has an onset time constant defined by the decline from peak to sustained firing rate, and an offset time course defined by the recovery function obtained by varying the time between the offset of the conditioning motion and the onset of the test motion.

The goal of the present series of papers was to use extracellular recording to constrain the mechanisms of this type of short-term adaptation in area MT. The data in the present paper address two possible classes of mechanisms: 1) input-specific mechanisms: adaptation in MT simply could be inherited from adaptation already present in the firing of its inputs or could be created by short-term depression in the synapses that transmit those inputs to MT. 2) Intrinsic spiking mechanisms of individual neurons: most excitatory neurons exhibit spike frequency adaptation for a step of input current so that the response consists of a transient that decays to a lower sustained firing rate. In the sections that follow, we will argue that our data render unlikely both of these possible explanations.

Input-specific mechanisms of adaptation

MT neurons receive a strong input from direction-selective neurons in V1, and most but not all of the direction-selective response of MT neurons disappear after V1 has been ablated (Rodman et al. 1989). Under the assumption that most of the driving input to MT comes from V1, we assessed the possibility of input-specific mechanisms of adaptation by evaluating the spatial extent of adaptation in MT. If adaptation arises in the inputs from V1, then the spatial scale of adaptation should be small: a conditioning motion presented at one location in the visual field should not cause adaptation to motion presented subsequently at a different location as long as the separation of the stimuli causes them to excite different neurons in V1. Our data were not consistent with this prediction: the adaptation field of MT neurons was as large or larger than the receptive field and adaptation generalized across locations roughly in proportion to the response evoked by the conditioning motion alone. Control experiments in V1 using the same spatial configuration of the conditioning and test motion failed to reveal evidence of adaptation in V1 that could be relayed to MT. Further, V1 neurons failed to show the same distribution of transient responses to moving stimuli that are the signature of adaptation in MT. We conclude that the short-term adaptation in MT is not inherited from V1 nor is it produced by the synapses from V1 neurons onto MT neurons.

MT receives inputs from areas other than V1, for example, area V2 (DeYoe and Van Essen 1985), the pulvinar, and the higher motion area MST. Because adaptation transferred over distances only slightly larger than the receptive field size of neurons in area MT, we think that MST is an unlikely candidate for the source of the adaptation signal. MST neurons have much larger receptive fields than do MT neurons, so the spatial extent for adaptation would need to be on the scale of those receptive fields and not the smaller spatial scale found in our sample of neurons. The spatial scale of adaptation also makes it unlikely that V2 is the source of short-term adaptation in MT neurons. Direction-selective V2 neurons have receptive fields that are

larger than the those in V1 but smaller than those in area MT: at an eccentricity of 10° , V2 receptive fields extend an average of 3.5° (Gattass et al. 1981). Further, the receptive fields of the subset of V2 neurons that project to area MT are probably still smaller than this (Roe and Ts'o 1995). Because the majority of the neurons reported here (57/67) showed a spatial transfer of adaptation using a separation of the conditioning and test motion of more than 2° , we think it is unlikely that V2 is providing the primary source of adaptation observed in area MT. We conclude that short-term adaptation probably occurs within MT but with the caveat that more information will be needed about response properties of pulvinar neurons that provide to MT before we can draw any conclusions about its possible role in adaptation.

Our data on the spatial transfer of adaptation in V1 and MT raise two important questions. First, if adaptation occurs within area MT, why did conditioning motions at many locations reduce but not abolish the transient response to the test motion? This result would be expected if adaptation is a consequence of the organization of the intracortical circuit in area MT and is based on the interaction of neurons with overlapping receptive fields. Conditioning motion at a location eccentric from the center of the receptive field may not affect the firing of all neurons that provide inputs to the neuron under study. Thus the conditioning motion will recruit only the portion of the circuit subserving the conditioning location: subsequent test motion will recruit some parts of the MT circuit where adaptation has occurred and others where it has not. Second, given that V1 neurons respond transiently to flashed bars (Kulikowski et al. 1979; Nelson 1991), why did we not observe transient responses in V1 neurons to our motion stimulus? A simple explanation for the lack of transient response in V1 neurons is that while MT neurons responded to the motion of the texture, V1 neurons responded to individual dots in the texture passing through their receptive fields. The dot density of our textures was $0.75 \text{ dot}/^\circ^2$, while the area of a receptive field of V1 neurons at the eccentricities we examined is about 0.25°^2 . Therefore our stimuli did not always place a moving dot in the receptive field of the neuron. Because the initial position of the dots was randomized across trials, the first dot would have started to traverse the receptive field of V1 neurons at a different time for each trial. Thus our data do not rule out the existence of adaptation to motion in V1. Rather through the use of a stimulus that was not suitable for generating adaptation in V1, we have been able to show the existence of a separate form of adaptation that seems to occur within MT.

Intrinsic spiking mechanisms of adaptation

When driven by a step of current injected by an intracellular microelectrode, cortical neurons show spike frequency adaptation (Connors and Gutnick 1990; McCormick et al. 1985). The resulting spike train is superficially similar to the response of an MT neuron to a step of target speed: it contains an initial transient that decays quickly to a lower sustained firing rate. One can think of many mechanisms for spike frequency adaptation, but the most prominent is driven by ion channels that react to the occurrence of a spike with an elevated K^+ conductance. This conductance decreases firing rate by deepening the afterhyperpolarization (AHP) that follows each action potential. In the absence of spikes, the AHP current decays gradually to its baseline with a time constant that would be compatible with the time course of recovery of adaptation in MT (Connors and Gutnick 1990; McCormick et al. 1985).

Our data fail to support any of three predictions of an intrinsic spiking mechanism of adaptation:

Prediction 1—If spiking causes adaptation, then conditioning motion should suppress the transient response to test motion only insofar as the conditioning motion evokes spikes. There was a strong correlation between the activity and the adaptation evoked by a given conditioning motion, but the relationship was not as tight as would be expected if spiking causes adaptation. For example, the adaptation fields of MT neurons were consistently somewhat larger than the receptive fields. Further, we saw examples of conditioning motion that caused adaptation

without evoking spikes, both in the present paper and the subsequent paper of this series (Priebe and Lisberger 2002).

Prediction 2—If spiking causes adaptation, then variability in the early transient across individual trials should cause correlated changes in the subsequent firing rate. In the 35 neurons where we had enough data to perform this analysis, we saw no such correlation.

Prediction 3—If there are zero spikes in the interval that normally has a transient response, then there should be a large transient response in the subsequent interval. Our analysis of 25 neurons failed to find any evidence for this prediction. Firing rate was typically unchanged or slightly lower than usual, not higher than usual, in the subsequent interval. We conclude that the spikes of an MT neuron do not cause short-term adaptation directly. Of course, adaptation could be caused by intrinsic mechanisms that operate at a subthreshold level, a possibility that will have to be tested with intracellular recordings. However, a subthreshold mechanism would have to satisfy the unlikely criterion of being uncorrelated with the neuron's suprathreshold activity to provide the basis for short-term adaptation.

Concluding statement

We have constrained the mechanism of short-term adaptation in visual area MT. If the adaptation occurs through an input-specific mechanism, then it must depend on inputs from areas other than V1 and probably V2. If the adaptation occurs through intrinsic cellular mechanisms, it cannot be tightly linked to the occurrence of spikes in the neuron. We have arrived at our conclusions through condition/test experiments in which two different motion components were presented in succession. Our approach and goals were different from those of other researchers, who have measured the effect of two distinct motions that occurred simultaneously inside the receptive fields of MT (Britten and Heuer 1999; Majaj et al. 2000). However, our conclusions agree with theirs, which is that a computational mechanism called “normalization” occurs in MT as well as possibly in other areas.

One function of normalization is to dilute the effect of changes in the overall level of inputs to a neuron on its output firing rate, while at the same time preserving response selectivity (Carandini et al. 1997). For example, normalization would make the coding of speed or direction in MT relatively insensitive to a reduction in the overall level of its inputs when contrast is reduced. If the time course of normalization was slower than that for direct neural responses, then normalization would cause the kind of adaptation we have analyzed here (Lisberger and Movshon 1999). Thus available data suggest that adaptation in area MT is a property of the intrinsic circuit within MT and arises from a circuit organization that implements normalization, as others have suggested (Britten and Heuer 1999; Majaj et al. 2000). The subsequent paper (Priebe and Lisberger 2002) constrains the organization of the adapting circuit by asking whether the inputs that drive adaptation are dependent on other properties of the adapting stimulus, such as its direction or speed of motion.

Acknowledgements

We are grateful to S. Ruffner for creating the target presentation software, to C. Cassanello and L. Osborne for participating in the experiments, and to K. MacLeod and E. Montgomery for assistance with animal preparation and maintenance. We thank J. Hanover, T. Movshon, K. Miller, M. Stryker, and J. Korenbrot for helpful discussions and comments.

Research was supported by the Howard Hughes Medical Institute and by National Eye Institute Grants R01-EY-03878 and T32-EY-07120.

References

- Allman J, Meizin F, McGuinness E. Stimulus specific responses from beyond the classical receptive field: neurophysiological mechanisms for local-global comparisons in visual neurons. *Annu Rev Neurosci* 1985a;8:407–430. [PubMed: 3885829]
- Allman J, Miezin F, McGuinness E. Direction- and velocity-specific responses from beyond the classical receptive field in the middle temporal visual area (MT). *Perception* 1985b;14:105–126. [PubMed: 4069941]
- Batschelet. *Circular Statistics in Biology*. London: Academic; 1981.
- Britten KH, Heuer HW. Spatial summation in the receptive fields of MT neurons. *J Neurosci* 1999;19:5074–5084. [PubMed: 10366640]
- Carandini M, Heeger DJ, Movshon JA. Linearity and normalization in simple cells of the macaque primary visual cortex. *J Neurosci* 1997;17:8621–8644. [PubMed: 9334433]
- Cavanaugh JR, Bair W, Movshon JA. Signals setting contrast gain arise from iso-oriented domains aligned with the receptive field axis of macaque striate cortex neurons. *Soc Neurosci Abstr* 1998;24:1875.
- Chance FS, Nelson SB, Abbott LF. Synaptic depression and the temporal response characteristics of V1 cells. *J Neurosci* 1998;18:4785–4799. [PubMed: 9614252]
- Churchland MM, Lisberger SG. Shifts in the population response in the middle temporal visual area parallel perceptual and motor illusions produced by apparent motion. *J Neurosci* 2001;21:9387–9402. [PubMed: 11717372]
- Connors BW, Gutnick MJ. Intrinsic firing patterns of diverse neocortical neurons. *Trends Neurosci* 1990;13:99–104. [PubMed: 1691879]
- DeYoe EA, Van Essen DC. Segregation of efferent connections and receptive field properties in visual area V2 of the macaque. *Nature* 1985;317:58 – 61. [PubMed: 2412132]
- Gattass R, Gross CG, Sandell JH. Visual topography of V2 in the macaque. *J Comp Neurol* 1981;201:519–539. [PubMed: 7287933]
- Gibson J, Radner M. Adaptation, after-effect and contrast in the perception of tilted lines. I. Quantitative studies. *J Exp Psychol* 1937;20:453–467.
- Hubel DH, Wiesel TN. Receptive fields and functional architecture in two non-striate visual areas (18 and 19) of cat. *J Neurophysiol* 1965;23:229–289. [PubMed: 14283058]
- Judge S, Richmond B, Chu F. Implantation of magnetic search coils for measurement of eye position: an improved method. *Vision Res* 1980;20:535–538. [PubMed: 6776685]
- Kaplan E, Mukherjee P, Shapley R. Information filtering in the lateral geniculate nucleus. *Contrast Sensitivity* 1993;5:183–199.
- Kayser A, Priebe NJ, Miller KD. Contrast-dependent, nonlinearities arise locally in a model of contrast-invariant orientation tuning. *J Neurophysiol* 2001;85:2130–2149. [PubMed: 11353028]
- Kilgard MP, Merzenich MM. Anticipated stimuli across skin. *Nature* 1995;373:663–663. [PubMed: 7854442]
- Knierim JJ, van Essen DC. Neuronal responses to static texture patterns in area V1 of the alert macaque monkey. *J Neurophysiol* 1992;67:961–980. [PubMed: 1588394]
- Kulikowski JJ, Bishop PO, Kato H. Sustained and transient responses by cat striate cells to stationary flashing light and dark bars. *Brain Res* 1979;170:362–367. [PubMed: 466416]
- Lisberger S, Movshon J. Visual motion analysis for pursuit eye movements in area MT of macaque monkeys. *J Neurosci* 1999;19:2224–2246. [PubMed: 10066275]
- Lisberger SG, Westbrook LE. Properties of visual inputs that initiate horizontal smooth pursuit eye movements in monkeys. *J Neurosci* 1985;5:1662–1673. [PubMed: 4009252]
- Majaj N, Smith MA, Movshon JA. Contrast gain control in macaque area MT. *Soc Neurosci Abstr* 2000;26:392.
- McCormick DA, Connors BW, Lighthall JW, Prince DA. Comparative electrophysiology of pyramidal and sparsely spiny stellate neurons of the neocortex. *J Neurophysiol* 1985;54:782–806. [PubMed: 2999347]

- Merrill EG, Ainsworth A. Glass-coated platinum-plated tungsten microelectrode. *Med Biol Eng* 1972;10:495–504.
- Mikami A, Newsome W, Wurtz R. Motion selectivity in macaque visual cortex. II. Spatiotemporal range of directional interactions in MT and V1. *J Neurophysiol* 1986;55:1328–1339. [PubMed: 3734858]
- Miller, RG. *Simultaneous Statistical Inference*. 2. New York: Springer-Verlag; 1981.
- Movshon JA, Newsome WT. Visual response properties of striate cortical neurons projecting to area MT in macaque monkeys. *J Neurosci* 1996;16:7733–7741. [PubMed: 8922429]
- Muller JR, Metha AB, Krauskopf J, Lennie P. Rapid adaptation in visual cortex to the structure of images. *Science* 1999;285:1405–1408. [PubMed: 10464100]
- Nelson SB. Temporal interactions in the cat visual system. I. Orientation-selective suppression in the visual cortex. *J Neurosci* 1991;11:344–356. [PubMed: 1992005]
- Priebe NJ, Lisberger SG. Constraints on the source of short-term motion adaptation in macaque area MT. II. Tuning of neural circuit mechanisms. *J Neurophysiol* 2002;88:370–382. [PubMed: 12091561]
- Rodman HR, Gross CG, Albright TD. Afferent basis of visual response properties in area MT of the macaque. I. Effects of striate cortex removal. *J Neurosci* 1989;9:2033–2050. [PubMed: 2723765]
- Roe AW, Ts'o DY. Visual topography in primate V2: multiple representation across functional stripes. *J Neurosci* 1995;15:3689–3715. [PubMed: 7751939]
- Saul A, Humphrey A. Spatial and temporal response properties of lagged and nonlagged cells in cat lateral geniculate nucleus. *J Neurophysiol* 1990;64:206–224. [PubMed: 2388066]
- Schrater P, Simoncelli E. Local velocity representation: evidence from motion adaptation. *Vision Res* 1998;38:3899–3912. [PubMed: 10211382]
- Softky WR, Koch C. Cortical cells should fire regularly, but do not. *Neural Comput* 1992;4:643–646.
- Sokal, RR.; Rohlf, FJ. *Biometry: The Principles and Practice of Statistics in Biological Research*. 3. New York: W. H. Freeman; 1995.
- Stevens, SS.; Davis, H. *Its Psychology and Physiology*. New York: Wiley; 1938. Hearing.
- Takeuchi T, De Valois KK, Motoyoshi I. Light adaptation in motion direction judgments. *J Opt Soc Am A Opt Image Sci Vis* 2001;18:755–764. [PubMed: 11318325]
- Tolhurst DJ, Walker NS, Thompson ID, Dean AF. Non-linearities of temporal summation in neurons in area 17 of the cat. *Exp Brain Res* 1980;38:431–435. [PubMed: 6244972]
- Victor JD. The dynamics of the cat retinal X cell center. *J Physiol (Lond)* 1987;386:219–246. [PubMed: 3681707]
- Walker GA, Ohzawa I, Freeman RD. Asymmetric suppression outside the classical receptive field of the visual cortex. *J Neurosci* 1999;19:10536–10553. [PubMed: 10575050]
- Wohlgenuth A. On the aftereffect of seen movement. *J Psychol* 1911;1:1–117.
- Zipser K, Lamme VA, Schiller PH. Contextual modulation in primary visual cortex. *J Neurosci* 1996;16:7376–7389. [PubMed: 8929444]

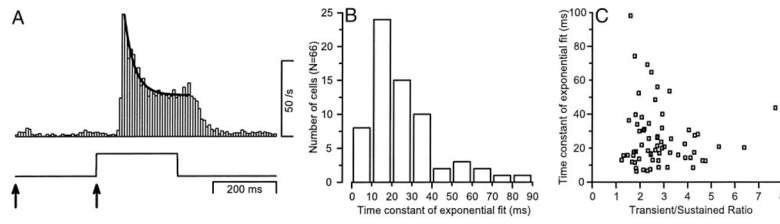


Fig. 1.

The response of an MT neuron to a step of image velocity and the transition from transient to sustained firing. *A*: firing rate histogram accumulated from the responses of an MT neuron to 265 repetitions of a 256-ms-duration step of target speed at $8^\circ/\text{s}$. Bin size is 8 ms, and the trace beneath the histogram shows the time course of stimulus speed. The bold line superimposed on the histogram shows a fit of the exponential described by Eq. 5 to the firing rate of the neuron. Values of the parameters were: τ , 31.1 ms; f_{max} , 80.7 spikes/s; f_{sus} , 27.5 spikes/s; T/S ratio, 2.9. *B*: histogram showing the distribution of the values of τ , the time constant of the exponential fits, for our sample population. Mean \pm SD of the sample were 25.9 ± 17.9 ms. *C*: scatter plot showing the absence of a relationship between the time constant of the transition from transient to sustained firing and the transient-sustained ratio for the MT neurons in our population. Each symbol plots data from a different neuron. One neuron was not included in this plot because it had an extraordinarily high transient-sustained ratio of 21. The time constant of the transition from transient to sustained firing was 22 ms for that neuron.

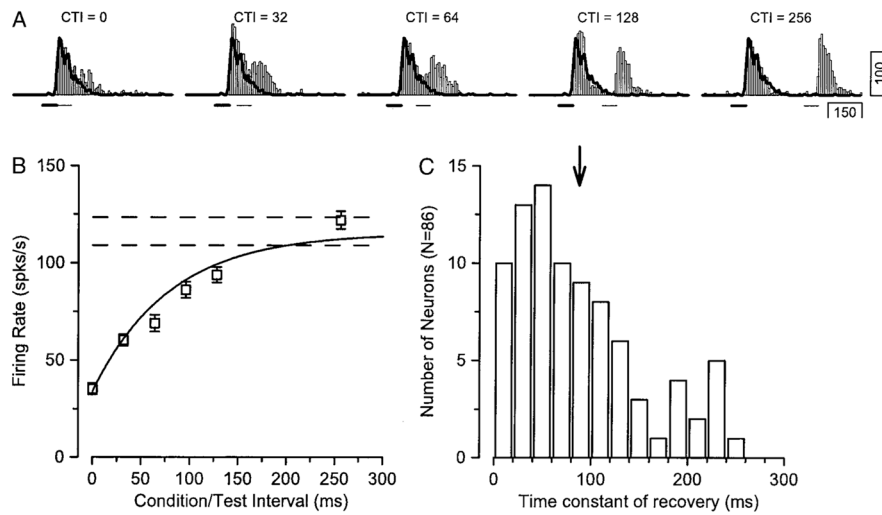


Fig. 2. The recovery of MT neurons from short-term adaptation. *A*: histograms of the firing rate of an MT neuron showing its response to 2 brief 64-ms-duration presentations of motion with different condition/test intervals (CTI). The bold trace superimposed on each histogram shows the response to the conditioning motion alone. The bold and fine horizontal lines below the histograms show the times of the conditioning and test motions, respectively. The test and conditioning motion were both in the preferred direction and at the preferred speed of the neuron. *B*: assessment of the time course of recovery from short-term adaptation by plotting the firing rate evoked by the test motion as a function of the condition/test interval. These values were measured from the difference firing rate obtained by subtracting the response to the conditioning motion alone from the response to the conditioning/test stimulus. The horizontal dashed lines indicate 95% confidence intervals for the response of the neuron to the test motion without preceding conditioning motion, estimated as the mean response ± 1 SE. The continuous curve indicates the exponential that provided the best fit to the recovery of the neuron. The time constant of recovery for this neuron was 73 ms. The error bars on the symbols indicate the standard error of the mean. *C*: histogram showing the distribution of the time constant of recovery for all the neurons in our sample population. The arrow indicates the mean recovery time constant of 86 ms.

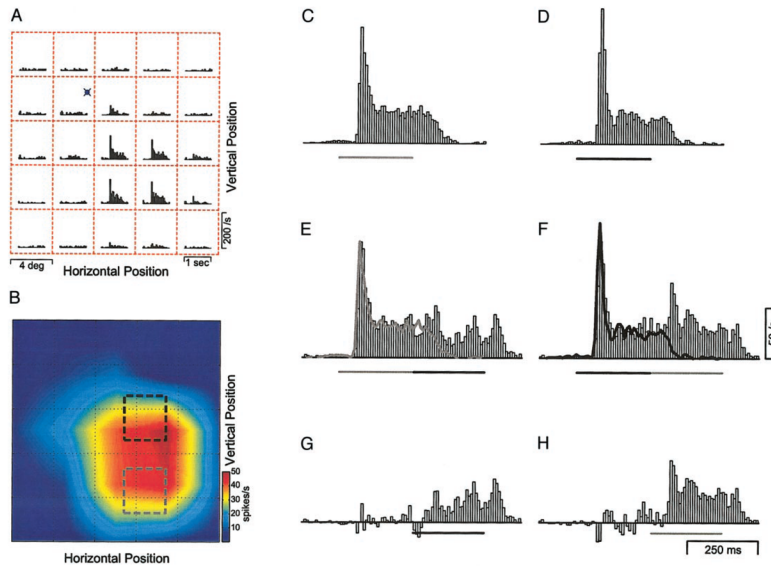


Fig. 3. Example of the transfer of adaptation across the spatial extent of an MT neuron's receptive field. *A*: each histogram shows the response of an MT neuron to motion placed in the portion of the visual field occupied by the histogram in the red grid. The texture appeared at the beginning of each trial, remained stationary for 256 ms, moved with the preferred speed and direction of the neuron for 512 ms, and was stationary again. The cross and circle indicate the location of the fovea. *B*: a pseudo-color representation of the spatial extent of the receptive field based on the histograms in *A*. Blue indicates low firing, and red indicates high firing. The gray and black dashed boxes indicate the locations used for the conditioning and test motions in experiments summarized by the rest of the figure. Fine dashed lines indicate position in 4° steps. *C* and *D*: histograms showing the responses of the neuron to testing motion in the area defined by the gray box (*C*) or the black box (*D*) alone. *E* and *F*: histograms showing the response of the neuron to motion in the gray box followed by the black box (*E*) or motion in the black box followed by motion in the gray box (*F*). The bold gray line in *E* and the bold black line in *F* show the responses to motion in the gray or black box alone, from *C* and *D*. *G* and *H*: difference firing rate obtained by subtracting the response to the conditioning motion alone from the response to conditioning/test motion. In *C-H*: the gray and black horizontal lines beneath the histograms indicate the duration of motion within the gray and black boxes, respectively.

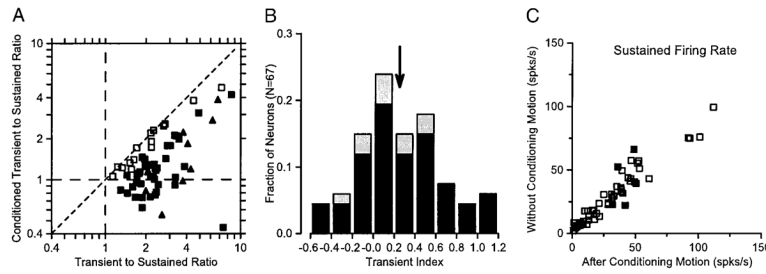


Fig. 4. Summary of the spatial transfer of adaptation within our sample of neurons. *A*: the transient-sustained ratio measured in the absence of conditioning motion is plotted relative to the transient-sustained ratio after conditioning motion in another portion of the receptive field. Each neuron contributed 2 points to show the effect of conditioning motion in each of the 2 stimulation locations on the response to test motion in the other. ■ and ▲, cases where the conditioning motion caused statistically significant changes in the transient response to subsequent test motion ($P < 0.05$, *t*-test). □ and ▼, cases that did not show a statistically significant effect. ■ and □ and ▲ and ▼ represent data recorded from anesthetized and awake animals, respectively. *B*: distribution of the value of the transient index (defined in Results) for all of the neurons in our sample. ■ and □, neurons recorded from the anesthetized and awake animals, respectively. *C*: scatter plot showing the mean sustained firing rate of each neuron to test motion without conditioning motion as a function of that after conditioning motion. ■ and □, cases with and without statistically significant effects of conditioning motion on the sustained response to test motion.

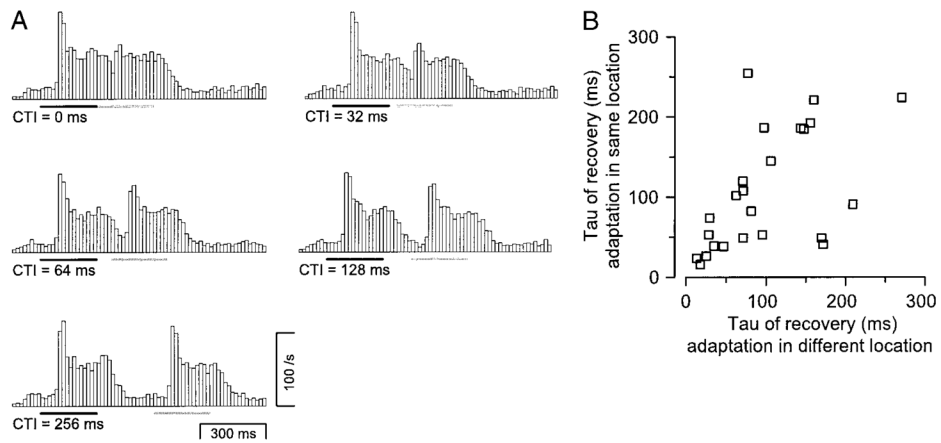


Fig. 5. The time course of recovery from adaptation. *A*: each histogram shows the response of an example neuron for a range of CTIs, using conditioning and test motions at separate locations. The black and gray horizontal lines under the histograms show the time and duration of the motion in the conditioning and test locations. *B*: time course of recovery when the conditioning and test locations were the same is plotted as a function of that when they were different. Each symbol summarizes the responses from 1 neuron.

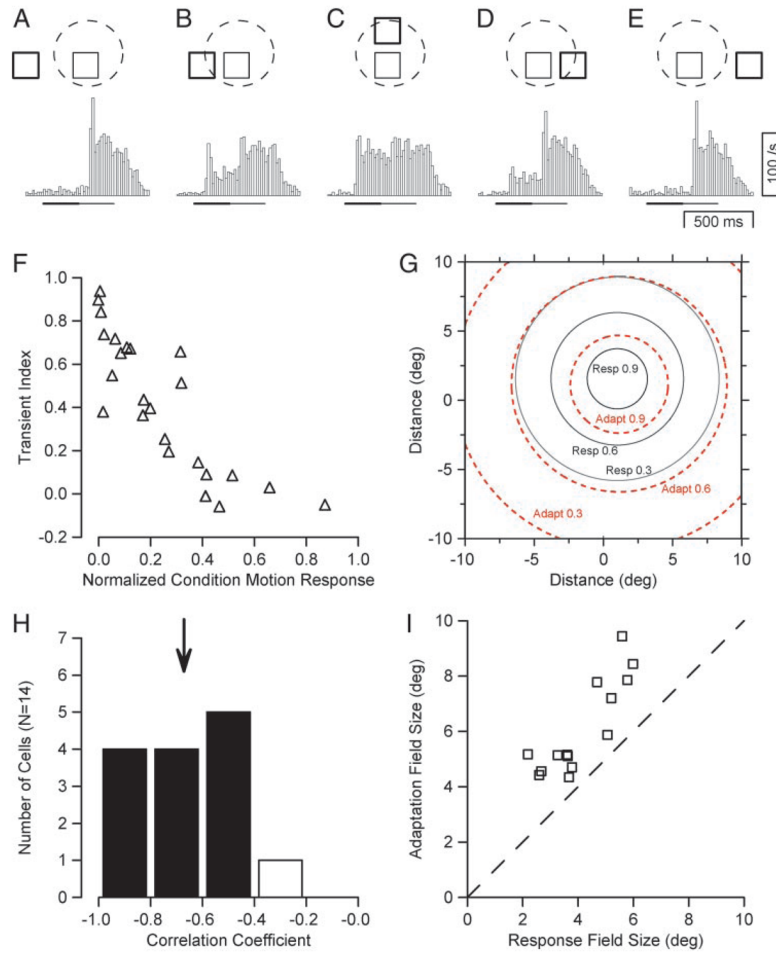


Fig. 6. Comparison of the size of response field and adaptation field. *A–E*: histograms showing the responses to test motion at the center of the receptive field following conditioning motion at different locations. In the diagram above each histogram, the dashed circle shows the receptive field of the MT neuron, the fine square indicates the location of the test motion, and the bold square shows the location of the conditioning motion. Each dot texture covered $4 \times 4^\circ$ and the distance between the centers of the conditioning and test textures were 11.3° (*A* and *E*) or 5.2° (*B–D*). *F*: summary of the relationship between the transient index for test motion following conditioning motion and the response to the same conditioning motion alone. All the data were taken from the example neuron used to create the histograms in *A–E*, and each symbol shows data for a single location of conditioning motion. *G*: solid and dashed contour circles summarize the Gaussian functions that best fit the response and adaptation fields, respectively. *H*: distribution of the correlation coefficients obtained by analysis of the relationships between the transient index and the response to the conditioning motion for our sample of 14 neurons. The arrow indicates the mean correlation for the sample. Filled and open bars indication correlations that were or were not statistically significant. *I*: scatter plot that compares the size of the adaptation and response receptive fields by plotting the value of sigma for the adaptation field as a function of that for the response receptive field. Each symbol shows data from 1 neuron. The dashed line indicates a slope of 1.

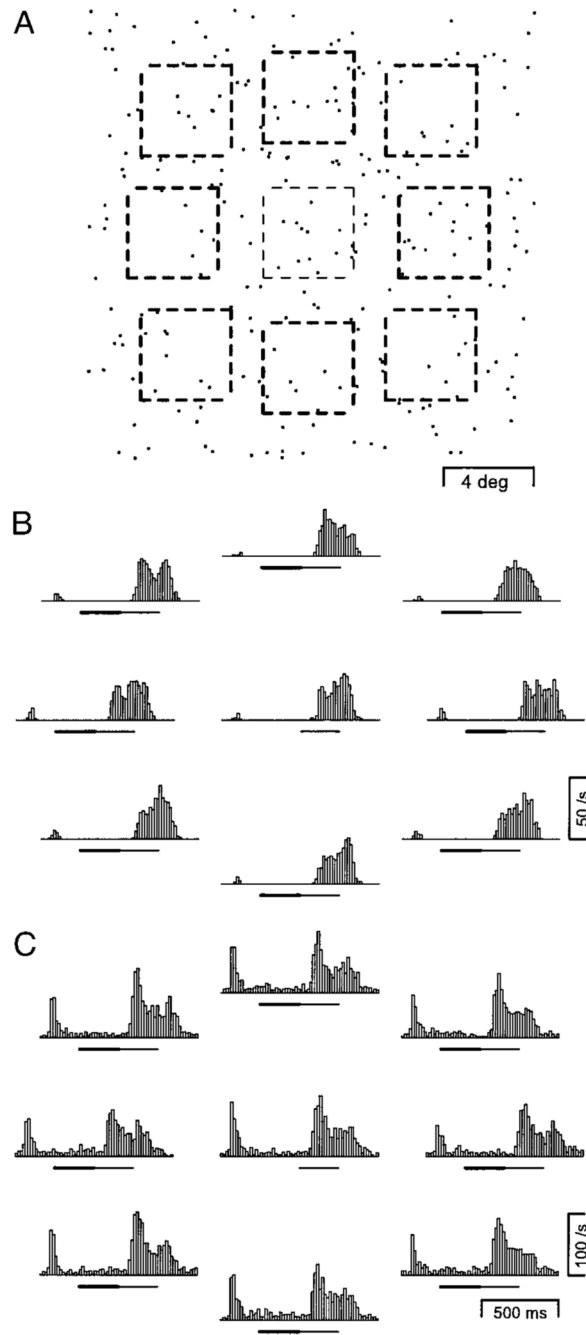


Fig. 7. The spatial transfer of adaptation in the primary visual cortex (V1). *A*: the stimulus arrangement used to study neurons in V1. The boxes outlined by thick and thin dashed lines indicate the locations of the conditioning and test motions. The dots have the same density used in these experiments. Dashed lines were not actually part of the display. *B* and *C*: the responses of 2 example neurons. The central histogram shows the response to test motion without preceding conditioning motion. The surrounding histograms indicate the responses to conditioning/test stimuli with the location of the conditioning motion indicated by the position of each histogram. The bold and fine horizontal lines below each histogram indicate the timing and duration of conditioning and test motion, respectively.

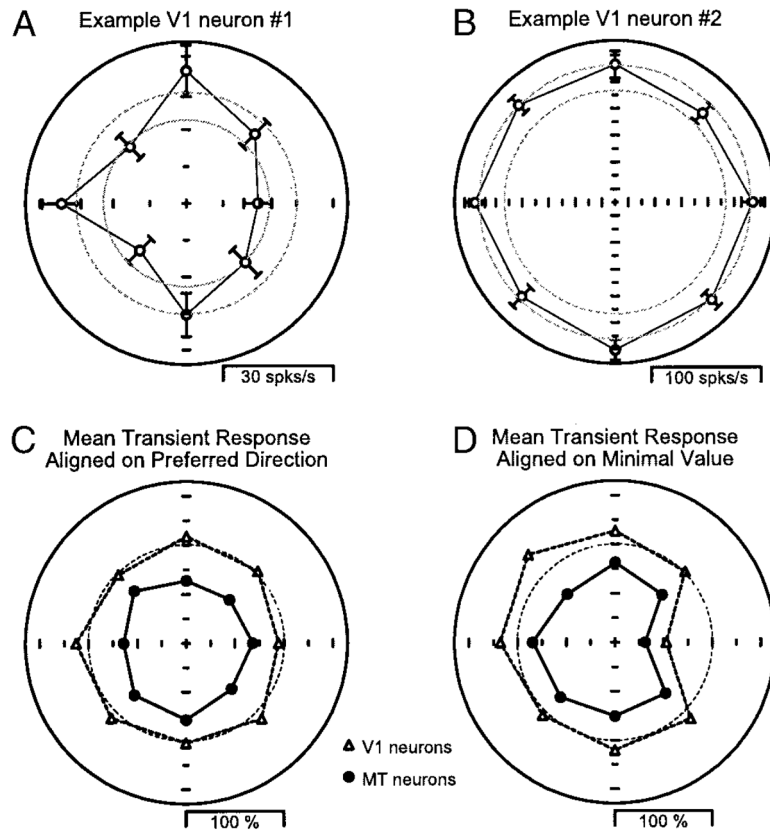


Fig. 8. Quantitative comparison of the spatial extent of adaptation in MT vs. V1 for the same stimulus configuration. *A* and *B*: the responses of 2 example neurons from V1. Each point is plotted in polar coordinates, where the distance from the origin indicates the size of the response to test motion after conditioning motion, and the angle indicates the position of the conditioning motion relative to the center of the receptive field. The 2 dashed circles indicate the 95% confidence interval for the response to test motion alone, estimated as the mean \pm 1 SE. The error bars on each symbol indicate the SE. Each tick along the horizontal and vertical axes represents 10 spikes/s. *C* and *D*: the mean response after conditioning motion is plotted as a function of the relative position of the conditioning stimulus, after rotating each neuron's data so that the preferred direction (*C*) or the greatest suppressed of the response (*D*) is plotted to the right. Open triangles and filled circles show responses for the sample of neurons recorded in V1 and MT, respectively. The dashed circle indicates a normalized transient response of 1.

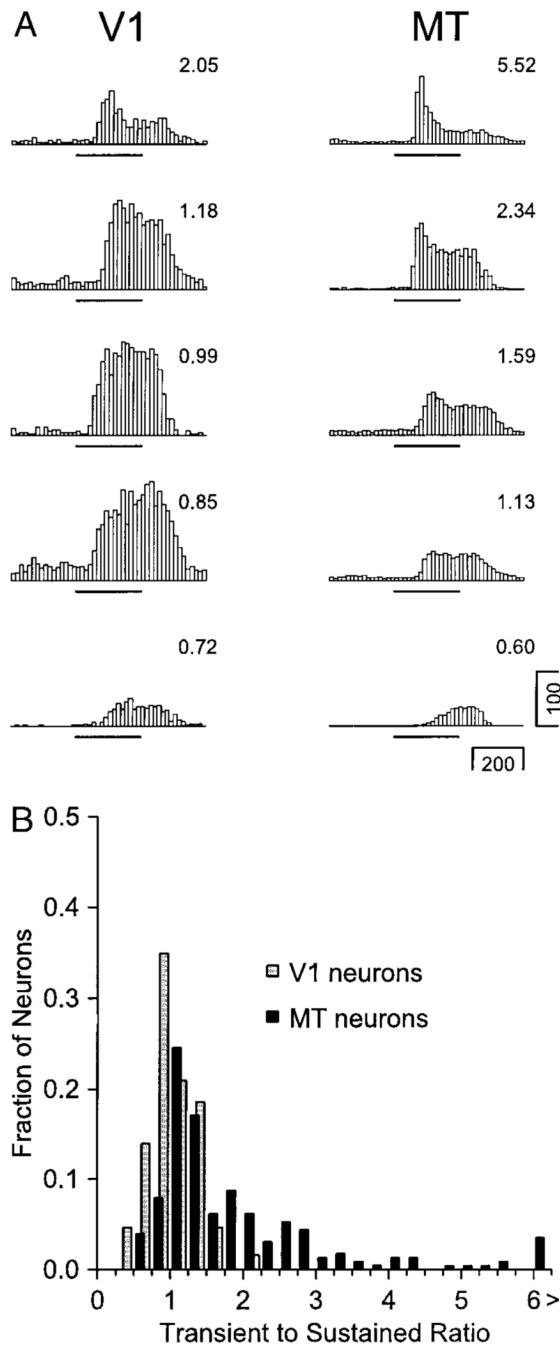


Fig. 9. Absence of transient responses in V1 neurons. *A*: examples of the spectrum of transient responses of V1 and MT neurons to steps of texture speed. — (below each histogram), the timing and duration of texture motion of the preferred direction and speed of the neuron being recorded. The number at the top right of each histogram indicates the transient-sustained ratio. *B*: quantitative comparison of the distribution of transient-sustained ratios in V1 and MT neurons. ■ and □, summary of our samples of 213 neurons in MT and 63 direction-selective neurons in V1, respectively.

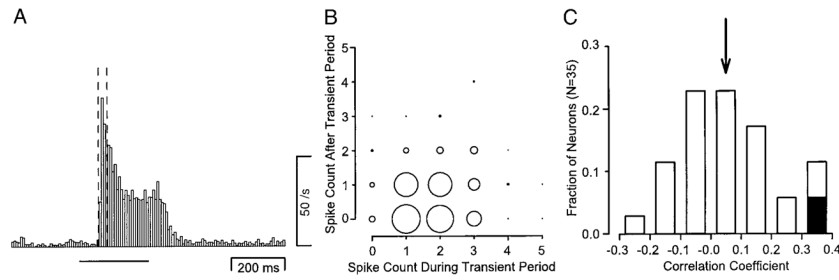


Fig. 10.

The effect of spiking activity during the transient period on subsequent firing. *A*: histogram showing the response of an MT neuron to a step of target speed accumulated in 8-ms wide bins from 265 repetitions of the preferred stimulus for the neuron under study. The 2 vertical dashed lines indicate the period defined from the average response as the transient period. The transient period is not aligned with the bins of the histogram because it was determined from separate analysis on a 1-ms time scale. *B*: the size of each circle summarizes the number of individual trials in which the number of spikes during transient interval and the subsequent 16 ms had the values indicated by the location of the circle on the *x* and *y* axes. The largest circle indicates a combination of transient and sustained spike counts that occurred in 45 different trials. *C*: the distribution of correlation coefficients from plots like that in *B* for the 37 neurons in our sample population. Filled and open bars indicate correlation coefficients that were or were not statistically significant (*t*-test, $P > 0.05$). The downward arrow above the histogram indicates the mean correlation coefficient in our sample, which was 0.05.

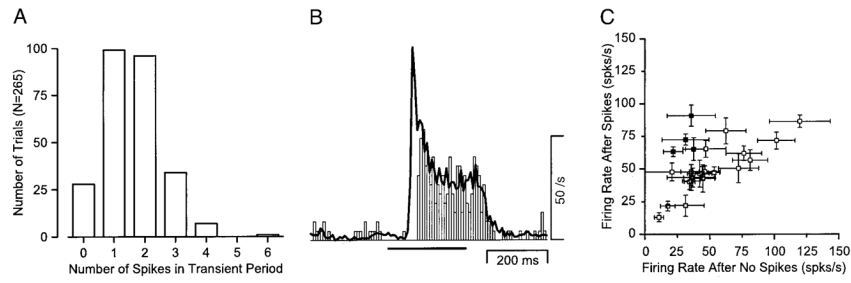


Fig. 11.

Comparison of time course of response in trials with and without spikes in the transient period defined from the average response. *A*: the frequency of different spike counts during the transient period for the same example neuron used to construct the histogram in Fig. 10A. *B*: the histogram shows the firing rate of the neuron for 26 trials that lacked spikes during the transient period defined from the average response. The thick trace shows the average response of the neuron for 239 trials in which 1 or more spikes occurred during the transient period. *C*: graph showing the effect of spiking during the transient interval on the adaptation of MT neurons. Each point plots data from 1 neuron. The y axis plots firing rate during the 16 ms after the transient interval when 1 or more spikes occurred in the transient interval. The x axis plots firing rate during the 16 ms after the transient interval when no spikes occurred in the transient interval defined from the average firing rate. Filled symbols indicate 4 neurons that showed statistically different responses under these 2 conditions, depending on the presence of spiking in the transient period. Horizontal and vertical error bars show the standard errors of the mean for the conditions of spiking or no spiking during the transient period.